Secondary ligands enhance affinity at a designed metal-binding site

Stephen F Marino and Lynne Regan

Background: Specific interactions of metal ions with proteins are central to all life processes. The varied functions enabled by this cooperation are a consequence of strict control of the binding-site environment, particularly the number, type and geometry of metal-coordinating sidechains. Attempts to mimic these characteristics in the *de novo* design of metal-binding sites have thus far concentrated primarily on metal recruitment and not on affecting site function through systematic fine-tuning of the metal environment.

Results: A designed tetrahedral Zn(II)-binding site in a variant of the B1 domain of IgG-binding protein G has been expanded by introducing 'secondary ligands'. These interactions were engineered to stabilize the positions of the metal-coordinating histidine residues while retaining the desired coordination geometry. Each mutation increased the protein's affinity for metal, and combining two secondary ligands demonstrated that these enhancements are additive. These results mimic the effects of altering similar interactions observed in the native Zn(II)-binding site of carbonic anhydrase. In the B1 system, this enhanced affinity for metal is observed despite a substantial decrease in protein secondary structure.

Conclusions: The intended effects of secondary ligand addition on metal affinity were observed in each mutant and demonstrated to be additive. Addition of metal also stabilized the protein's structure, partially offsetting the destabilizing effect of the mutations. These results represent a successful first attempt at designing an extended metal-binding site environment and illustrate the importance of including secondary interactions in the design of metal-binding sites.

Address: Department of Molecular Biophysics and Biochemistry, Yale University, 266 Whitney Avenue, New Haven, CT 06520, USA.

Correspondence: Lynne Regan
E-mail: lynne@csbgly.csb.yale.edu

Key words: cobalt, folding, metal binding, protein design, zinc

Received: **1 June 1999**
Accepted: **21 June 1999**

Published: **12 August 1999**

Chemistry & Biology September 1999, **6**:649–655
http://biomednet.com/elecref/1074552100600649

1074-5521/99/$ – see front matter

Introduction

Because of the fundamental importance of protein–ligand interactions to every biological process, much effort in the field of protein design has focused on both the engineering of new binding functions into proteins and the rational modification of existing interactions. Because of their simplicity as modeled ligands and the wealth of structural and biochemical data available for native systems, metal ions have been the target ligands in a number of successful design studies (reviewed in [1,2]). Such work has produced metal-binding systems with diverse functions including protein purification [3–5], modulation of protein function, structure and stability [6–13], and membrane channel gating [14]. Although the introduction of functional binding moieties has been repeatedly demonstrated, there has been less success in constructing 'native-like' sites — those with the specific coordination geometries and/or site architecture seen in natural metalloproteins [15,16]. The highly organized binding context that is a hallmark of native sites must be reproduced in designed sites intended for the more precise and sensitive functions required of catalysts or metal ion biosensors. Including such considerations in the design process will lead to sites whose properties can be 'tuned' to suit the requirements of different applications [17].

The biological importance of Zn(II) as a required cofactor for multiple classes of proteins is well documented [18]. This fact, coupled with the wealth of structural information available for Zn(II) proteins, makes the rational design of native-like Zn(II)-binding sites a tractable goal. Whether as a structural component or as the center of enzymatic activity, Zn(II) coordination by proteins is predominantly with tetrahedral geometry [19,20]. In addition to the direct metal–sidechain interactions, there are also extensive hydrogen-bonding networks that serve to stabilize the positions of the metal-coordinating sidechains [21]. Previous studies of such interactions in the Zn(II) metalloenzyme carbonic anhydrase focused on the systematic alteration of the 'second shell' metal ligands — the sidechain hydrogen-bonding partners of the metal-binding site histidine residues [22,23]. This work demonstrated that decreasing the entropy of the coordinating histidine sidechains through interaction with hydrogen-bonding partners could result in up to a tenfold increase in affinity for metal per interaction. Given this dramatic effect on

metal-binding and the prevalence of these interactions in both structural and catalytic metal sites, the importance of their consideration in site design is obvious.

Building on the successful design of a tetrahedral Zn(II)-binding site in a variant of the B1 domain of protein G (the Zβ1 family of proteins) [24], we sought to rationally increase metal affinity by introducing 'secondary ligand' interactions to stabilize the conformations of the metal-coordinating histidine sidechains. Several residues adjacent to the metal-binding site were chosen for introducing acidic and amide sidechains positioned for potential hydrogen–bonding interactions with δ or ε histidine nitrogens. All of the resulting proteins do display enhancements in affinity for metal with each secondary ligand incorporation despite the surprising observation that the scaffold domain—in some cases, even in the presence of metal—appears largely unfolded. A possible explanation for this behavior is discussed.

Results and discussion

The system

The starting point of this study was a designed Zn(II)-binding site in a variant of the B1 domain of IgG-binding protein G (Figure 1). A tetrahedral His_3Cys site was introduced between the α helix and second β strand of this 56-residue domain. Initial modeling of the site identified a potential steric overlap between Leu5 in the hydrophobic core and His30 in the helical portion of the proposed binding site. Residues considered as a replacement for Leu5 were modeled into the protein and three variants were ultimately chosen—alanine, methionine or the wild-type leucine. The three resulting metal-binding domains were designated Zβ1A, Zβ1M and Zβ1L based on these replacements. All three of these proteins bound Co(II) with micromolar affinity and the intended tetrahedral geometry. The Leu5 variant Zβ1L was chosen for further study because it retained the most wild-type structure and stability as assessed by circular dichroism (CD) and nuclear magnetic resonance (NMR).

Figure 1

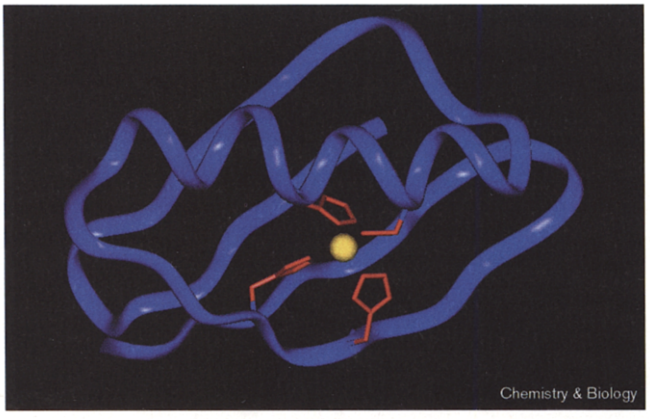

Ribbon model of Zβ1L showing the binding-site residues His16, His18, His30 and Cys33 (red), and Zn(II) ion (yellow).

Figure 2

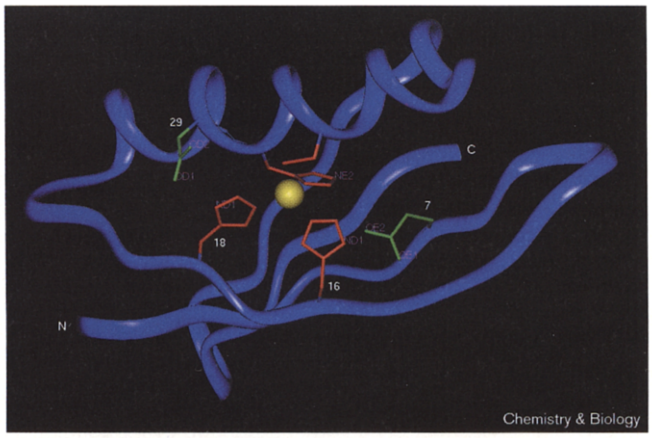

Ribbon model of Zβ1L showing the binding-site residues (red), Zn(II) ion (yellow), and positions of secondary ligands L7E/Q and V29D/N(green).

Having generated a site with the desired binding characteristics, we sought to improve the design by incorporating secondary ligands to effect improvements in the site affinity for metal. Inspection of the Zβ1L model identified three positions for mutation that would place nearly isosteric sidechains within hydrogen-bonding distance of nitrogens on all three of the coordinating

Figure 3

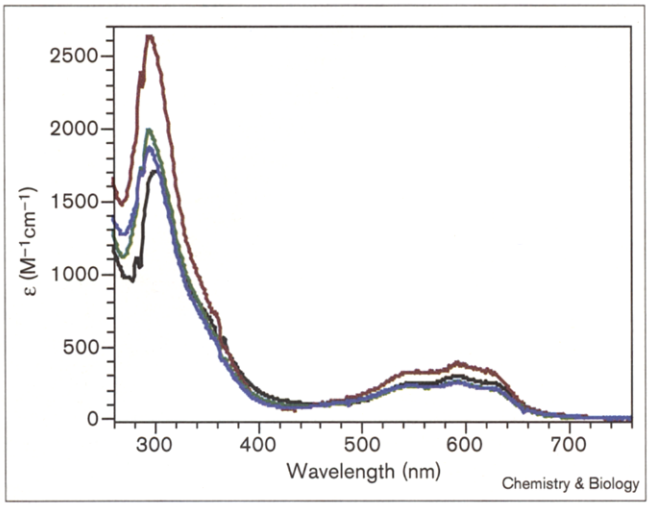

Representative spectra of the Co(II) complexes of Zβ1L (black) and secondary ligand mutants V29D (red), V29N (green) and V54D (blue). Displayed spectra are of proteins in the presence of saturating amounts of Co(II) and are corrected by subtraction of the spectrum of the corresponding protein in the absence of metal.

Figure 4

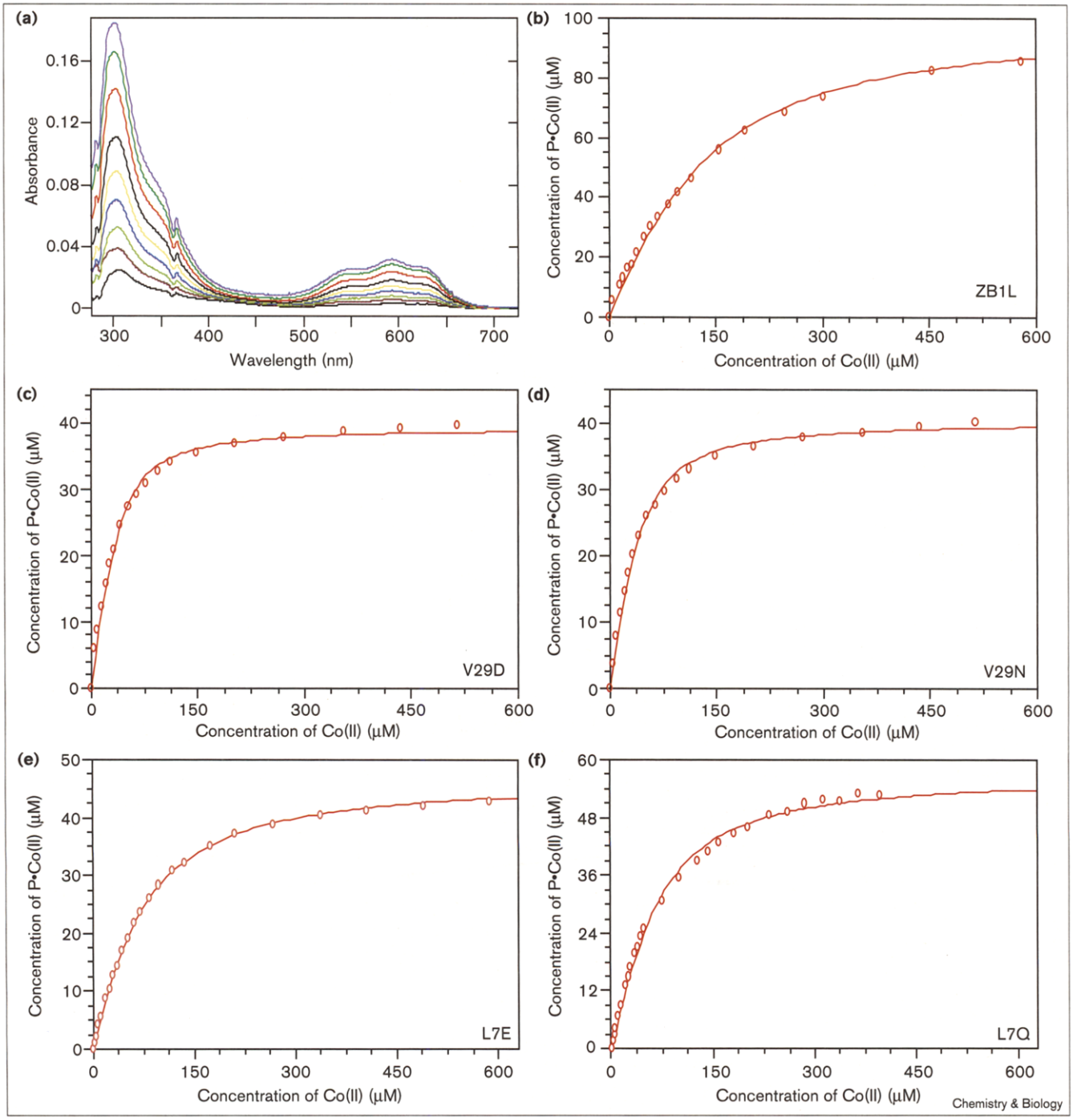

(a) Representative titration spectrum series showing the increase in absorbance upon successive additions of Co(II) to reduced, metal-free Zβ1 protein. The increase in absorbance at 298 nm was used to generate the binding curves for determining metal affinities.

(b–f) Co(II) titration curves of Zβ1L and single secondary-ligand mutants, plotting concentration of metal-complexed protein against total Co(II) concentration. Resulting curves were fit to the dissociation constant equation to determine the value of K_d.

imidazole rings. These were Leu7→Glu/Gln(L7E/Q) for interaction with the δnitrogen of His16, Val29→Asp/Asn(V29D/N) with the δnitrogen of His18 and Val54→Asp/Asn(V54D/N) with the εnitrogen of His30 (Figure 2). All mutants were constructed using cassette mutagenesis and were purified as previously reported for Zβ1L (with the exception of the Val54→Asn mutant, which failed to express).

Table 1

Co(II) affinities and λ_{max} extinction coefficients for Zβ1L secondary ligand mutants.

Protein	K_d (μM)	ε_{298}	ε_{592}
Zβ1L (wild type)	72.1 ± 3.5	1689	291
V29D	11.3 ± 2.5	2612	383
V29N	15.0 ± 4.8	1943	256
L7E	47.2 ± 11.8	1571	212
L7Q	34.2 ± 3.3	2105	298
V54D	28.7 ± 4.2	1946	243
L7E/V29D	8.0 ± 0.14 (~7.5)*	2319	349
L7E/V29N	16.2 ± 7.8 (~10)*	1483	215

*Additive affinity values predicted from the measured enhancements of the respective single mutants.

Metal binding

As a probe of the composition and geometry of metal sites specific for the spectroscopically silent Zn(II) species, absorption spectroscopy using Co(II) as ligand is commonly employed [25]. Metal d–d orbital transitions in ligated Co(II) result in an envelope of absorption peaks in the visible region of the absorption spectrum. The position of these peaks reflect the identities of the metal-coordinating atoms and the magnitude of the extinction coefficient at λ_{max} reflects the coordination geometry. To assess the sites of the Zβ1L secondary ligand mutants, purified apo-proteins were reconstituted with Co(II). In all cases, the absorption spectra displayed Co(II) d–d transition peaks with a λ_{max} of 592 nm with extinction coefficients ranging from 215 to 382 $M^{-1}\,cm^{-1}$. This λ_{max} is consistent with an N_3S donor set and the peak intensities are consistent with tetrahedral geometry, confirming that metal coordination in the mutants remains unchanged and that the complement of ligands at the binding site is likely identical to that in the parent molecule, Zβ1L (Figure 3). Dissociation constants were measured by metal titrations of all the mutants, and were performed by following the increase in absorbance of the cysteine sulfur to metal charge transfer peak at 298 nm as a function of Co(II) concentration (Figure 4). Affinity increases were seen for all five of these mutants and ranged from 1.5- to 6.4-fold greater than the 72 μM measured for Zβ1L (Table 1).

Because multiple interactions should have an additive effect on metal affinity [23], double mutants were constructed incorporating secondary ligands at Leu7 and Val29 together — L7E/V29D and L7E/V29N. Co(II) titrations did indeed show further increases in binding affinity for these double mutants, close to the values predicted based on the effect of each single mutant (Figure 5). Together, these mutations increase the affinity of the original designed site by nearly an order of magnitude, from about 72 μM to less than 8 μM. Although the magnitude of the increase for the L7E/V29D mutant was too great to give more than a lower limit using our Co(II) absorbance assay, the observed changes in affinity are consistent with the addition of the intended interactions and correspond closely to the affinity changes observed in the analogous studies of carbonic anhydrase [23].

Structure

Although the mode of metal binding has apparently been preserved and the expected affinity enhancements have been measured, the CD spectra of the single mutants (Figure 6) unexpectedly show little secondary structure. In the presence of metal however, all of the mutants show enhanced ellipticity, with the Leu7 mutants showing the most significant increases. In the case of the double mutants, the CD spectra show slightly enhanced secondary structure content as compared to the single mutants both with and without added metal. Metal-induced precipitation of concentrated samples has complicated the interpretation of one-dimensional ^1H NMR spectra beyond the observation that significant broadening of the resonances occurs in the presence of metal (data not shown). Although the effect of metal on the spectra may indicate some structural

Figure 5

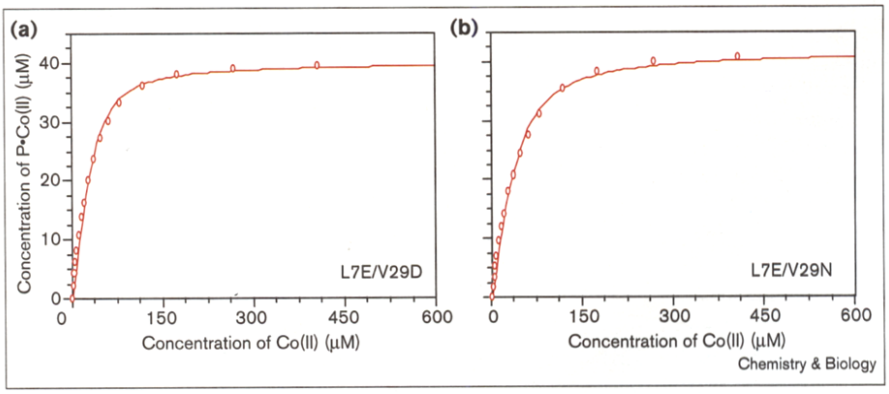

Co(II) titration curves of double secondary ligand mutants.

Figure 6

Circular dichroism spectra of **(a)** V29D, **(b)** V29N, **(c)** L7E and **(d)** L7Q secondary-ligand mutants in the presence (solid symbols) and absence (open symbols) of one molar equivalent of Zn(II).

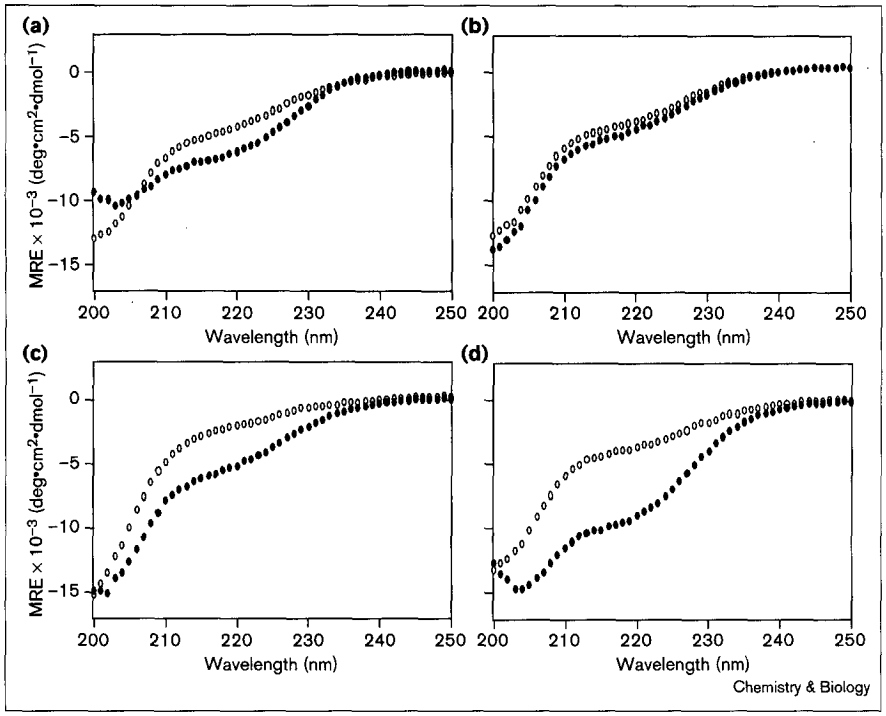

rearrangement consistent with the CD data, even the metal-free spectra do not provide evidence for the presence of a single, stably folded species. Taken together the data indicate that these proteins apparently possess little of the structure and stability of the Zβ1L parent, even though their affinities for metal have improved.

Despite these changes in secondary structural content, Figure 3 clearly demonstrates that the Co(II) spectra of all mutants display the same absorption envelope, suggesting that metal-ion interaction at the designed site remains unchanged. This loss of structural integrity is surprising, given the retention of coordination geometry and the enhanced affinity of metal binding.

Preservation of metal binding

Although the structure of the original scaffold has been altered, the architecture of the metal site has apparently been preserved. Given these observations, identifying the cause(s) of the increases in metal affinity, whether entropic or electrostatic, is not straightforward. The CD spectra of all of the mutants indicate some enhancement of secondary structure upon metal addition. In considering metal binding, the double mutants do show further affinity enhancements over the single mutants, which, in the absence of high-resolution structural data, is the most direct evidence obtainable that the intended interactions occur. In order to understand the unexpected structural behavior of the secondary-ligand mutants, it is instructive to look more closely at the relation of the altered residues to the integrity of the native protein.

The residues that were altered in this study (with the exception of Val29) all make hydrophobic contacts with other β1 core residues and are important for the stability of the wild-type B1 domain [26,27]. Although mutation of these residues in Zβ1L results in structural perturbation, in every case this effect leaves the binding site apparently unperturbed and increased affinity for metal is observed. Altering these sidechains then, although affecting the stability of the domain, obviously does not prevent proper positioning of the metal-coordinating residues. This may be explained, at least in part, by the proximal location of the relevant residues as illustrated in Figure 7.

The positions of the metal site histidine and cysteine residues lie on β-strand 2 (His16 and His18) and on the α helix (His30 and Cys33), which are connected by a two-residue turn (Val21–Asp22). Because His16 and His18 lie on an extended strand, the minimal structural requirement for the positioning of site residues would be formation of the α helix, which is necessary for fixing the relative positions of His30 and Cys33. Having preorganized these two residues, all that remains for metal binding is to bring the histidine sidechains from the adjacent strand into a proximal position. Therefore, assuming that the secondary-ligand mutations don't disrupt helix formation, there is no obvious impediment to site formation in the presence of metal. It is relevant to note that studies on the denatured state of the wild-type B1 domain have identified conformationally restricted segments of the protein corresponding to the residues in the strand 2/helix turn as well as within the

Figure 7

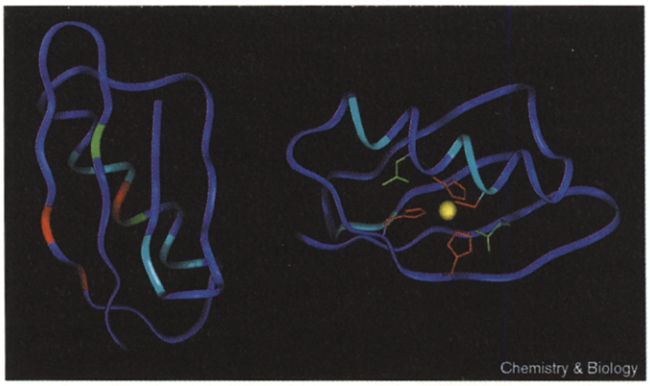

Ribbon diagrams of Zβ1L showing the positions of the binding site residues (red) and secondary ligands (green) with respect to the positions determined to have high ^{1}H-^{2}D exchange protection factors (cyan) taken from [29].

helix itself [28]. These results are in good agreement with the high amide ND-NH protection factors determined for several helix residues early in folding [29], identifying the helix as the potential 'folding nucleus' of the B1 domain.

Interactions with secondary ligands

Although the low stability of the mutants prevents the direct identification of the intended hydrogen-bonding interactions, our data strongly suggest that the measured increases in metal affinity are due to the secondary ligands. Consider first the mutants at Val29. Val29 is adjacent to the metal site His30 on the α helix and is completely exposed to solvent in the wild-type domain. Because it is situated on the helix, its position relative to the metal site is fixed upon helix formation and no large structural changes would be necessary in the presence of metal to bring it into proximity with its hydrogen-bonding partner, His18. In fact, there is no substantial difference in the CD spectra of this mutant with and without metal (Figure 6). In addition, the V29D mutant shows the largest increase in metal affinity — more than sixfold over Zβ1L. By contrast, the mutants at Leu7 — which is completely buried in the wild-type domain — place polar sidechains in the hydrophobic core of the protein. The CD spectra of the apo forms of these mutants indicate less structured species than those of the Val29 mutants — especially for the L7E mutant, which buries a full negative charge. Interaction of this sidechain on β-strand 1 with its intended partner, His16 on β-strand 2, would potentially require fixing the position of the entire strand1/strand2 hairpin with respect to the helix. The CD spectra of the Leu7 mutants in the presence of metal ions do indeed show a larger increase in ellipticity than that seen in the Val29 mutants (Figure 6), consistent with this scenario. The more modest increase in metal affinity of the Leu7 single mutants as compared to that of the Val29 mutants presumably reflects the energetic cost of fixing the strand1/strand2 hairpin, with consequent burial of polar sidechains, for proper metal binding. The same interpretation holds for the behavior of the single buried mutant of Val54 with respect to the strand3/strand4 hairpin (data not shown).

Even more compelling, the addition of two secondary ligands together results in a further increase in the site affinity for metal, of the order expected based on the carbonic anhydrase study of Kiefer *et al.* [23]. Combining the 6.4-fold enhancement of the V29D mutation (Co(II) affinity 11.3 μM) with the 1.5-fold enhancement of the L7E mutation (Co(II) affinity 47.2 μM) gives a double mutant with a predicted affinity of 7.5 μM — in good agreement with the measured affinity in excess of 8 μM. In addition, the CD spectra of this double mutant demonstrate similar behavior of this protein to that seen with the L7E mutation alone: little secondary structure in the apo form, with a comparable ellipticity increase in the presence of metal. Taken together, these data provide strong support for attributing the observed increases in metal affinity to the engineered secondary-ligand interactions.

Significance

The broad range of activities exhibited by metals in biological systems makes them attractive targets for protein design efforts. To date, a number of published studies have successfully demonstrated simple recruitment of metal to engineered sites. The challenge of constructing sites for more complex properties such as catalysis or sensor applications, however, requires a method for reproducing the precise balance of interactions that are observed in native metal sites. The work presented here represents the second stage in the stepwise design of a native-like metal-binding site. Building on our previous construction of a Zn(II) site with specified coordination geometry, we have now enhanced its affinity for metal by introducing 'secondary ligands'. These mutations provide the stabilizing hydrogen-bonding partners for the metal-chelating histidine sidechains that are observed in natural metalloproteins and allow us to rationally alter metal-binding properties. Comparison of our results with studies of these interactions in the active site of carbonic anhydrase underscores the necessity of including secondary ligands as an additional design criterion for the successful engineering of native-like metal-binding sites.

Materials and methods

Materials

All mutants were cloned by insertion of DNA cassettes prepared with polymerase chain reaction (PCR) primers containing the specified mutations. Mutagenic oligonucleotides were prepared on an Applied Biosystems 392 DNA synthesizer using standard phosphoramidite chemistry. The codons corresponding to the secondary ligand positions were synthesized with a mixture of nucleotides at the first position in order to generate a pool of mutant primers containing codons for both the specific acidic amino acid residues and their amide counterparts at those positions ([G/A]AC for aspartate and asparagine, and

[G/C]AA for glutamate and glutamine). Mutant sequences were verified via dideoxy DNA sequencing and the resulting proteins were grown and purified using the protocol devised for Zβ1L reported previously [24]. Concentrations were determined using the extinction coefficient at 280 nm (ε_{280}) of 8560 M^{-1} cm^{-1} determined for Zβ1L.

Computer graphics

Computer graphics models and figures were produced on a Silicon Graphics workstation using the program Insight (BioSym). Curve fits and plots were produced using the program Kaleidagraph (Abelbeck Software).

Circular dichroism

All spectra were collected on an Aviv 62DS spectrometer in 2 mm pathlength cells at 4°C using 20 μM samples in buffer containing 1 mM MOPS (American Bioanalytical), 0.1 mM tricarboxyethylphosphine (TCEP), (Pierce), pH 6.8. Protein samples with and without added $ZnCl_2$ (Aldrich) were prepared anaerobically in a glove box (see below) by reduction with dithiothreitol (DTT) (American Bioanalytical) followed by desalting into the MOPS/TCEP buffer. Spectra are the average of three scans.

Co(II) titrations

Protein for metal titrations was prepared under nitrogen by incubation with excess DTT and desalting by passage over a Sephadex G-25M column (PD-10, Pharmacia) into buffer containing 20 mM HEPES (Boehringer–Mannheim) pH 7.5. All solutions were degassed by two cycles of freezing in liquid nitrogen, pumping under vacuum and thawing and were stored under nitrogen. Titrations were performed in an anaerobic gas mixture (90% N_2, 5% CO_2, 5% H_2) in septum-sealed cuvettes, in duplicate, with sequential additions of aliquots of an ~5 mM stock solution of $CoCl_2$ (Aldrich) made via 10 and 100 μl Hamilton syringes. All metal stock solution concentrations and total Co(II) concentration, $[Co]_T$, in all assays were determined by flame atomic absorption spectrometry using a Varian SpectrAA-20 instrument. Protein concentrations before, during and after each titration were determined on stock solution samples by titration of the single cysteine residue with 5,5′-dithiobis-2-nitrobenzoic acid (DTNB) (Aldrich) and in all cases agreed with the values calculated by absorbance at 280 nm to between 2 and 11%. Only DTNB-derived values were used in fitting the data. Collected spectra were corrected for dilution and baseline offset and protein–metal complex concentrations, [P*Co], were calculated according to:

$$(\Delta A_{298}/\Delta A_{298}\text{max})[P]_T$$

where $[P]_T$ is the DTNB-derived protein concentration, ΔA_{298} is the measured increase in absorbance after each Co(II) addition, and ΔA_{298}max is the absorbance change at saturation determined by linear extrapolation of a plot of $1/\Delta A_{298}$ versus $1/[Co(II)]_T$. For each data set, the dissociation constant (K_d) was determined by quadratic fit of the data to the rearranged expression:

$$K_d = ([P]_T - [P^*Co])([Co]_T - [P^*Co]) / [P^*Co]$$

where $[P]_T$ is the total protein concentration as above, $[Co]_T$ is the total Co(II) concentration and [P*Co] is the concentration of metal-complexed protein. Titration curves were fit allowing both $[P]_T$ and K_d to vary and best fits to the data consistently gave protein concentration values ~10% below the DTNB values. This deviation was seen consistently with all of the proteins measured and is apparently inherent to the assay. Because DTNB assays could only be performed on samples of protein stock in the absence of metal, one possible explanation for the deviation may be loss of protein – for example, due to low levels of precipitation (though not apparent) – during the course of the titrations.

Acknowledgements

We thank Edgardo Farinas and Indraneel Ghosh for critical review of the manuscript and insightful discussion. This work was supported by the Office of Naval Research (N00014-95-1-0913) and by the C.E. Culpeper Foundation.

References

1. Regan, L. (1995). Protein design: novel metal binding sites. *Trends Biochem. Sci.* **20**, 280-285.
2. Hellinga, H.W. (1998). The construction of metal centers in proteins by rational design. *Fold. Des.* **3**, R1-R8.
3. Ljungquist, C., *et al.*, & Nilsson, B. (1989). Immobilization and affinity purification of recombinant proteins using histidine peptide fusions. *Eur. J. Biochem.* **186**, 563-569.
4. Arnold, F.H. & Haymore, B.L. (1991). Engineered metal-binding proteins: purification to protein folding. *Science* **252**, 1796-1797.
5. Müller, H.N. & Skerra, A. (1994). Grafting of a high-affinity Zn(II)-binding site on the β-barrel of retinol-binding protein results in enhanced folding stability and enables simplified purification. *Biochemistry* **33**, 14126-14135.
6. Corey, D.R. & Schultz, P.G. (1989). Introduction of a metal-dependent regulatory switch into an enzyme. *J. Biol. Chem.* **264**, 3666-3669.
7. Ghadiri, M.R. & Choi, C. (1990). Secondary structure nucleation in peptides. Transition metal ion stabilized α-helices. *J. Am. Chem. Soc.* **112**, 1630-1632.
8. Kellis, J.T.J., Todd, R.J. & Arnold, F.H. (1991). Protein stabilization by engineered metal chelation. *Bio/Technology* **9**, 994-995.
9. Handel, T.M., Williams, S.A. & DeGrado, W.F. (1993). Metal ion-dependent modulation of the dynamics of a designed protein. *Science* **261**, 879-887.
10. Matthews, D.J. & Wells, J.A. (1994). Engineering an interfacial zinc site to increase hormone-receptor affinity. *Chem. Biol.* **1**, 25-30.
11. Willett, W.S., Gillmor, S.A., Perona, J.J., Fletterick, R.J. & Craik, C.S. (1995). Engineered metal regulation of trypsin specificity. *Biochemistry* **34**, 2172-2180.
12. Elling, C.E., Nielsen, S.M. & Schwartz, T.W. (1995). Conversion of antagonist-binding site to metal-ion site in the Tachykinin NK-1 receptor. *Nature* **374**, 74-77.
13. Tian, Z.-Q. & Bartlett, P.A. (1996). Metal coordination as a method for templating peptide conformation. *J. Am. Chem. Soc.* **118**, 943-949.
14. Braha, O., *et al.*, & Bayley, H. (1997). Designed protein pores as components for biosensors. *Chem. Biol.* **4**, 497-505.
15. Chakrabarti, P. (1989). Geometry of interaction of metal ions with sulfur-containing ligands in protein structures. *Biochemistry* **28**, 6081-6085.
16. Chakrabarti, P. (1990). Geometry of interaction of metal ions with histidine residues in protein structures. *Protein Eng.* **4**, 57-63.
17. Christianson, D. & Fierke, C. (1996). Carbonic anhydrase: evolution of the zinc-binding site by nature and design. *Accounts Chem. Res.* **29**, 331-339.
18. Coleman, J.E. (1992). Zinc proteins: enzymes, storage proteins, transcription factors, and replication proteins. *Annu. Rev. Biochem.* **61**, 897-946.
19. Vallee, B.L. & Auld, D.S. (1990). Zinc coordination, function, and structure of zinc enzymes and other proteins. *Biochemistry* **29**, 5647-5659.
20. Vallee, B.L. & Falchuk, K.H. (1993). The biochemical basis of zinc physiology. *Phys. Rev.* **73**, 79-117.
21. Christianson, D.W. & Alexander, R.S. (1989). Carboxylate-histidine-zinc interactions in protein structure and function. *J. Am. Chem. Soc.* **111**, 6412-6419.
22. Lesburg, C.A. & Christianson, D.W. (1995). X-ray crystallographic studies of engineered hydrogen bond networks in a protein zinc-binding site. *J. Am. Chem. Soc.* **117**, 6838-6844.
23. Kiefer, L.L., Paterno, S.A. & Fierke, C.A. (1995). Hydrogen bond network in the metal binding site of carbonic anhydrase enhances zinc affinity and catalytic efficiency. *J. Am. Chem. Soc.* **117**, 6831-6837.
24. Klemba, M., Gardner, K.H., Marino, S.F., Clarke, N.D. & Regan, L. (1995). Novel metal-binding proteins by design. *Nat. Struct. Biol.* **2**, 368-373.
25. Bertini, I. & Luchinat, C. (1984). High spin cobalt(II) as a probe for the investigation of metalloproteins. *Adv. Inorg. Chem.* **6**, 71-111.
26. Gronenborn, A.M., *et al.*, & Clore, G.M. (1991). A novel, highly stable fold of the immunoglobulin binding domain of streptococcal protein G. *Science* **253**, 657-661.
27. Gronenborn, A.M., Frank, M.K. & Clore, G.M. (1996). Core mutants of the immunoglobulin binding domain of streptococcal protein G: stability and structural integrity. *FEBS Lett.* **398**, 312-316.
28. Frank, M.K., Clore, G.M. & Gronenborn, A.M. (1995). Structural and dynamic characterization of the urea denatured state of the immunoglobulin binding domain of streptococcal protein G by multidimensional heteronuclear NMR spectroscopy. *Protein Sci.* **4**, 2605-2615.
29. Kuszewski, J., Clore, G.M. & Gronenborn, A.M. (1994). Fast folding of a prototypic polypeptide: the immunoglobulin binding domain of streptococcal protein G. *Protein Sci.* **3**, 1945-1952.